PROBING STELLAR EXPLOSIONS WITH RADIOACTIVE BEAMS AT ORNL

MICHAEL S. SMITH

Physics Division, Oak Ridge National Laboratory, MS-6354, Bldg. 6010, P.O. Box 2008, Oak Ridge, TN 37831-6371, USA

E-mail: msmith@mail.phy.ornl.gov

Measurements of nuclear reactions on radioactive isotopes are necessary to understand stellar explosions such as novae and X-ray bursts. We have recently measured the $^{17}F(p,p)^{17}F$, $^{17}F(p,\alpha)^{14}O$, $^{18}F(p,p)^{18}F$, and $^{18}F(p,\alpha)^{15}O$ excitation functions with beams of radioactive ions produced at the Holifield Radioactive Ion Beam Facility (HRIBF) at Oak Ridge National Laboratory. Our experimental setup includes a Silicon Detector Array and the Daresbury Recoil Separator coupled to a windowless, differentially-pumped hydrogen gas target system. We have also measured the $^{12}C(p,\gamma)^{13}N$ cross section to commission our recoil separator for proton capture reactions on radioactive isotopes. To support these measurements, we are making unique calculations of isotope synthesis in stellar explosions to determine the effect of nuclear physics uncertainties on explosion model predictions. We are also making detailed evaluations of some nuclear reactions rates that are important input for explosion models.

1 Physics Motivation

There are a number of important astrophysical events during which hydrogen serves as fuel for (i.e., is burned by) (p,γ) fusion reactions under non-hydrostatic equilibrium conditions. These explosive hydrogen burning events, which include novae and X-ray bursts, are among the most energetic explosions (~10^{38} – 10^{45} ergs) known in the universe. Furthermore, these explosions affect the evolution of binary star systems and synthesize some of the elements comprising our bodies and the world around us. For these reasons, they have been the international focus of observational and theoretical efforts, as well as of laboratory measurements of the nuclear reactions that occur in (and sometimes drive) the explosions.

Nova explosions are accretion-driven phenomena, caused by the transfer of mass from one star to a compact white dwarf companion. The mass transfer and subsequent rise in temperature and pressure can initiate a runaway thermonuclear explosion, resulting in the synthesis of heavy elements (to mass ~ 40) and subsequent ejection into space. These catastrophic stellar events are characterized by extremely high temperatures and densities – greater than 10^8 K and 10^3 g/cm^3, respectively. Such conditions enable (p, γ) and (α,p) reactions to rapidly (on timescales of ns - min) produce unstable nuclei on the proton-rich side of the valley of stability. Any such nuclei (which decay via e^+-emission) produced with half-lives longer than, or comparable to, the mean time between nuclear reactions will become targets for subsequent nuclear processing. Sequences of (p, γ) and (α,p) reactions on *proton-rich radioactive nuclei* therefore occur during these explosions [1,2] and

produce abundances which are very different than those from the hydrogen burning occurring in non-explosive environments.

Indeed, observations of nova outbursts have revealed an elemental composition that differs markedly from solar [3,4]. Recent theoretical studies indicate that these differences are caused by the combination of convection with explosive hydrogen burning in the degenerate layer on the surface of a white dwarf star [5]. This results in a unique nucleosynthesis that is rich in odd numbered nuclei such as ^{13}C, ^{15}N, and ^{17}O which are difficult to form in other astrophysical environments. Some of the radioactive nuclei (those with lifetimes longer than 100 s) synthesized in explosions may be carried by convection to the top of the envelope before they decay (and make a small contribution towards powering the expansion [6]). Observations of the γ-ray lines (especially the 511-keV emission of ^{18}F) resulting from such radioactive decays in the envelope may provide stringent tests of nova models [7,8,9].

These γ-ray emissions depend sensitively on the amount of radionuclides synthesized by nuclear reactions in the explosion, which in turn depends on the rates of nuclear reactions driving the explosion [10,11]. Recently, it was shown that changes in the reaction rates used within a nova simulation had significant effects on both the production of individual isotopes (which can change by orders of magnitude in some cases) and on the peak luminosity and mass of ejected material [12]. Another study determined that the amount of observable ^{18}F surviving the nova thermonuclear runaway and transported into the envelope is severely constrained by the rates of nuclear reactions which destroy ^{18}F [9]. Current nova models also have difficulty reproducing global observables. For example, predictions of the mass of ejected material are in some cases a factor of 10 smaller than observations [13], and improved reaction rates will help quantify this problem.

Other accretion-driven phenomena important in astrophysics include X-ray bursts and X-ray pulsars. These can occur when material is accreted onto the surface of a neutron star, where temperatures and densities can reach over 10^9 K and 10^6 g/cm^3, respectively [14,15]. The ensuing explosive hydrogen burning can synthesize isotopes with masses up to masses 80 – 100 or beyond [15,16,17]. Recent studies of nucleosynthesis in these violent explosions suggest that their X-ray luminosity is influenced by the nuclear reactions (most involving proton-rich radioactive isotopes) used in the model [18].

There are also other astrophysical sites [16] – e.g., the accretion disk around black holes [19] – where nuclear reactions on proton-rich radioactive isotopes may play an important role. Critical comparisons of models for any of these sites with observations require a knowledge of the rates of *nuclear reactions on radioactive isotopes*. Measurements of such reactions have been, until recently, impossible due to the lack of intense radioactive nuclear beams. Models therefore employ reaction rate estimates based on systematic properties of nuclear states, on information from analogue nuclei, on partial resonance information from stable beam transfer reaction studies, and on statistical model calculations. For rates dominated by resonances, these estimates can be incorrect by orders of magnitude [2], and therefore the model

predictions of isotope synthesis and energy generation are necessarily uncertain. The recent development of radioactive beams has initiated a new era in laboratory nuclear astrophysics – one in which previously unattainable cross sections of nuclear reactions of astrophysical importance can be measured and subsequently incorporated into an emerging generation of sophisticated, computationally intensive models of stellar explosions.

Since numerous (p,γ) and (α,p) reactions on radioactive isotopes are thought to play an important role in stellar explosions, simulations have been used to determine which reactions are most important to measure. These simulations indicate that nuclear burning occurs through the Hot CNO cycles, including reaction sequences such as $^{12}C(p,\gamma)^{13}N(p,\gamma)^{14}O(e^+\nu_e)^{14}N(p,\gamma)^{15}O(e^+\nu_e)^{15}N(p,\alpha)^{12}C$ and $^{16}O(p,\gamma)^{17}F(p,\gamma)^{18}Ne(e^+\nu_e)^{18}F(p,\alpha)^{15}O$ [1,20]. Nuclei may be processed out of the Hot CNO cycles to isotopes with masses greater than 20 via reaction sequences such as $^{15}O(\alpha,\gamma)^{19}Ne(p,\gamma)^{20}Na(p,\gamma)^{21}Mg\ldots$, $^{18}F(p,\gamma)^{19}Ne(p,\gamma)^{20}Na(p,\gamma)^{21}Mg\ldots$, or $^{18}Ne(\alpha,p)^{21}Na(p,\gamma)^{22}Mg\ldots$. These can lead to hydrogen burning through the rapid proton capture process (rp-process) [1,20], involving (p, γ) reactions near the proton drip line competing with e^+ - decay and reaction cycles (e.g., the Ne-Na and Mg-Al cycles). At very high temperatures characteristic of X-ray bursts and X-ray pulsars ($T_9 \sim 1.5$, where we define T_9 as $T(K) / 10^9$ K), the reaction sequence $^{12}C(p,\gamma)^{13}N(p,\gamma)^{14}O(\alpha,p)^{17}F(p,\gamma)^{18}Ne(\alpha,p)^{21}Na(p,\gamma)^{22}Mg\ldots$ is the trigger for the (α,p)-process, which transitions into the rp-process at approximately mass 40 [15, 19]. The viability of any of these sequences depends on the rates of the reactions involved, and those on proton-rich radioactive isotopes have the largest uncertainties. These sequences are important because they increase the energy generation rate compared to non-explosive burning while simultaneously altering the abundances (e.g., the ratio of nitrogen and oxygen isotopes) that are synthesized.

The reactions $^{14}O(\alpha,p)^{17}F$, $^{17}F(p,\gamma)^{18}Ne$, $^{18}F(p,\gamma)^{19}Ne$, and $^{18}F(p,\alpha)^{15}O$ play an important role in the sequences discussed above. For these reasons, we have studied these reactions via experiments with radioactive beams at ORNL's Holifield Radioactive Ion Beam Facility (HRIBF) to better determine their rates at temperatures corresponding to stellar explosions.

2 The Holifield Radioactive Ion Beam Facility (HRIBF)

The HRIBF [21] is the only U.S. user facility producing and accelerating beams of proton-rich radioactive heavy ions using the Isotope Separator On-Line (ISOL) technique. To date, radioactive beams of ^{17}F, ^{18}F, $^{69,70}As$, and $^{66,67}Ga$ have been produced at the HRIBF; intensities of the fluorine beams were as high as a few million per second on target. Beams of ^{56}Ni and ^{7}Be are under development, and tests are beginning with a uranium carbide target to produce beams of neutron-rich radioactive isotopes. Radioactive ions are produced when a high-temperature (1100 - 2200° C), thin, refractory target [22] is bombarded by a 0.5 kW light ion (p, d, ^3He,

or ^{4}He) beam from the K=105 Oak Ridge Isochronous Cyclotron (ORIC). For example, fibrous Hf_2O_3 targets [23] are being used to produce ^{17}F via the ^{16}O(d,n)^{17}F reaction at 45 MeV and to produce ^{18}F via the ^{16}O(α,pn)^{17}F reaction at 85 MeV. This target material was chosen because of its high surface area to volume ratio and low density (enhancing diffusion of radioactive isotopes) and high melting point to withstand intense light-ion bombardment. A number of novel target configurations for high-efficiency release of radioactive isotopes are currently in use, and others are under design [22]. Once produced, the radioactive isotopes thermally diffuse out of the hot target material and effuse through a short (10 cm) transfer tube to an ion source for ionization and extraction. The particular ion source used is chosen to maximize the extracted radioactive species. An electron beam plasma ion source [23] has been used to produce positively-charged radioactive isotopes of F, As, and Ga, and a surface ionization source has been used to produce negatively-charged radioactive isotopes of F [24]. Once produced, the radioactive ions are then charge-exchanged (if they are positive ions) in a Cs vapor cell, then undergo two stages of mass separation (with the second having $\Delta M / M \leq 0.5 - 1 \cdot 10^{-4}$). They are then injected into the 25-MV tandem accelerator, accelerated to the energies needed for experiments (typically 0.2 - 2 MeV/u for astrophysics studies), and delivered to the experimental areas. Radioactive ion beams produced at the HRIBF have a number of important characteristics which make them well suited for nuclear astrophysics studies: high isobaric purity, good energy resolution, low emittance, low energies, and relatively high intensities.

3 Experimental Equipment

Once the radioactive beams are produced, they are directed to an experimental station dedicated to nuclear astrophysics measurements. This station consists of a Silicon Detector Array (SIDAR) installed in a large target chamber, followed by the Daresbury Recoil Separator (DRS), a large mass separator optimized for measurements of capture reactions in inverse kinematics.

3.1 SIDAR

The SIDAR, located in a large (40 cm diameter) target chamber upstream of the DRS, consists of up to 3 annular arrays of highly-segmented transmission silicon detectors (similar to those in refs. [25,26]) coupled to high-density, low-noise electronics. It is optimized for use in coincidence measurements of excitation functions and angular distributions of scattering, transfer, and (p,α) reactions in inverse kinematics with radioactive ion beams. These measurements are being used to precisely determine the properties of resonances which dominate reactions of astrophysical interest at energies relevant to stellar explosions. For some experiments (e.g., (p,α) reactions), the annular arrays in the SIDAR are used to

detect both light-ion and heavy-ion products of these reactions. In other experiments (e.g., (p,p) reactions), the SIDAR is used to detect light-ion products of nuclear reactions while the heavy ions are detected by a gas ionization counter located directly behind the SIDAR. The ionization counter is also used to monitor the intensity of the radioactive ion beam – because Faraday cups are ineffective at these currents – as well as the beam purity.

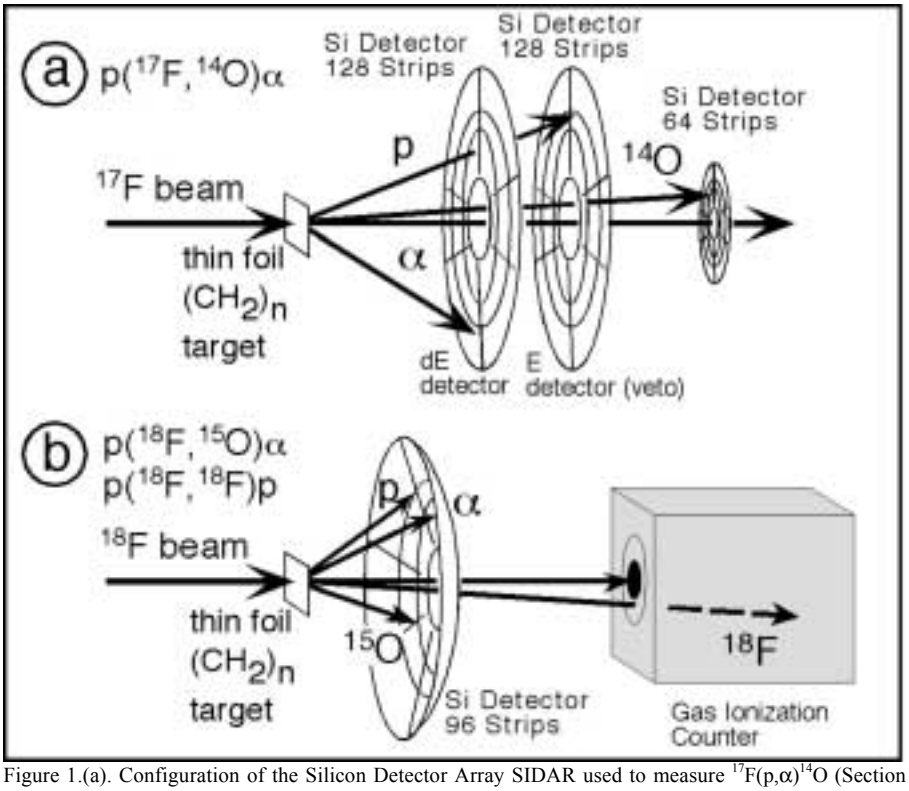

Figure 1.(a). Configuration of the Silicon Detector Array SIDAR used to measure $^{17}F(p,\alpha)^{14}O$ (Section 4.2) with two stacked 128-strip detectors (for light ions) backed by a 64-strip detector (for heavy ions). (b) SIDAR configuration used for $^{18}F(p,p)^{18}F$ and $^{18}F(p,\alpha)^{15}O$ with an angled 96-strip followed by a gas ionization counter.

A variety of mounting configurations of these transmission silicon strip detectors (including normal to the beam axis, angled toward the beam axis, and stacked for particle identification) have been developed and used (Figure 1). The solid angle coverage differs for each configuration, but typically values of 25 % are achieved – corresponding to an even higher detection efficiency for some reactions because of the kinematic focussing of the light ions. Relatively low radioactive ion beam intensities (~10^4 – 10^6 s^{-1}) can be utilized for many of these measurements, as

described in Section 4. The $^{17}O(p,p)$ and $^{17}O(p,\alpha)$ cross sections have been measured to commission the SIDAR for radioactive ion beam measurements [27].

3.2 Daresbury Recoil Separator

The Daresbury Recoil Separator (DRS) has been installed at the HRIBF and optimized for measuring capture reactions in inverse kinematics using a radioactive ion beam incident on a hydrogen or helium target. It is a large-acceptance (6.5 msr, ± 2.5 % in velocity), high-mass resolution (1 part in 300), 90-ton, 13-meter long device. It features two long (1.2 meter), crossed electric and magnetic field velocity filters, followed by a 50° dipole magnet that gives a mass/charge final focus [28]. Details of the installation of the DRS at ORNL can be found in refs. [29,30].

To determine the yield of a capture reaction, the DRS will be used to separate beam particles passing through the target from the products of the capture reaction. This approach, while challenging, has a number of advantages over more traditional capture γ ray detection techniques [29,31]. The recoil detection technique for proton capture reactions was first proven viable with a measurement of the $p(^{12}C,^{13}N)\gamma$ reaction with a relatively small, non-optimized recoil separator at Caltech [31]. In that work, a suppression of scattered beam particles – defined by the ratio of beam particles reaching the focal plane to those incident on the target – of 10^{-10} was obtained. At the HRIBF, a measurement of the $p(^{12}C,^{13}N)\gamma$ reaction was made with the DRS, using a 0.666 MeV/u ^{12}C beam incident on a CH_2 target. The DRS was tuned to focus the recoiling ^{13}N particles on the focal plane detectors – a carbon-foil microchannel plate detector (providing timing and position signals) followed by a gas ionization counter (providing particle identification). The (non-optimized) suppression of the scattered beam particles was measured to be $3 \cdot 10^{-11}$, within the 10^{-10} to 10^{-12} range needed for capture reactions with cross sections of ~ 1 μb. Furthermore, the gas ionization counter cleanly separated (i.e., with no overlap) the energy-loss (Bragg) curves of the low-mass, low-energy carbon and nitrogen particles above 0.4 MeV/u (Figure 2). In this first test, the combined projectile rejection of the DRS and the focal plane detector was well beyond that needed for capture reactions. Further commissioning tests are planned to optimize these results and to determine the transmission through the DRS.

Current tests with the DRS have used polypropylene (CH_2) foil targets. However, gas targets are preferred over foil targets because they have higher yields for the same target (energy loss) thickness, they have no background from carbon-induced reactions, they have no physical degradation or hydrogen-depletion problems common to CH_2 foils, and they enable measurements of alpha-induced reactions [(α, γ) and (α, p)] when helium is used. Therefore, a windowless, differentially-pumped hydrogen and helium gas target system is under construction, similar to that used in ref. [32].

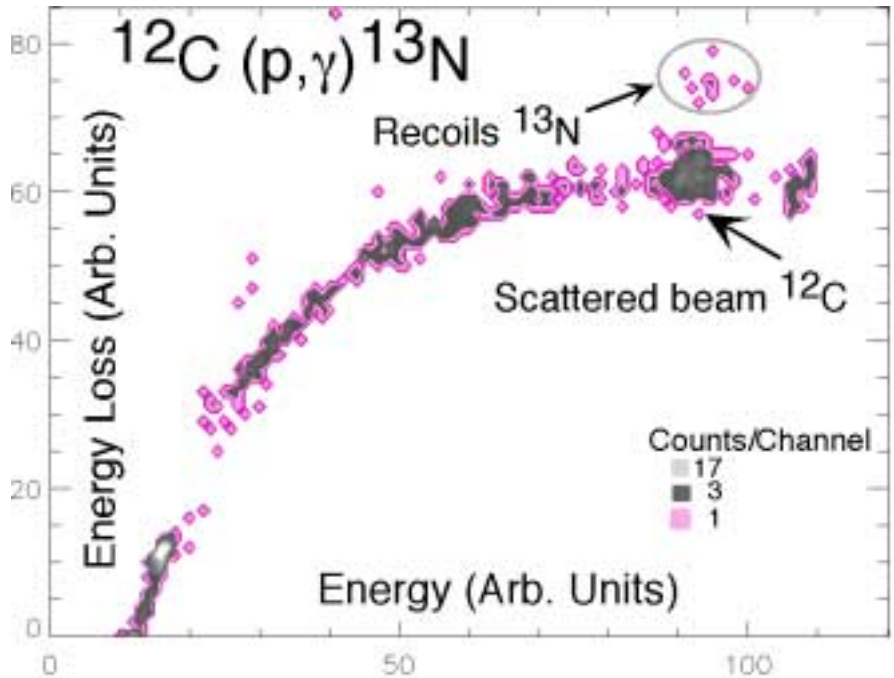

Figure 2. Identification of particles reaching the gas ionization counter at the DRS focal plane in a measurement of the $^{12}C(p,\gamma)^{13}N$ reaction.

4 Recent Radioactive Beam Measurements

4.1 The $^{14}O(\alpha, p)^{17}F$ Reaction

The rate of the $^{14}O(\alpha,p)^{17}F$ reaction depends critically on properties of states in the compound nucleus ^{18}Ne. In particular, a single $J^{\pi} = 1^-$ state near $E_x = 6$ MeV and its interference with the direct reaction cross section may dominate the reaction rate at temperatures $T_9 < 1$ [33, 34]. Despite recent studies of ^{18}Ne using both stable beams [34] and a ^{17}F beam [35], the rate of the $^{14}O(\alpha,p)^{17}F$ reaction remains very uncertain due to the unknown total and alpha-partial widths of the $J^{\pi} = 1^-$ resonance, the non-resonant reaction component, and the sign of the interference between resonant and non-resonant contributions. We have studied the $^{1}H(^{17}F,\alpha)^{14}O$ reaction, the time-inverse of the $^{14}O(\alpha,p)^{17}F_{gs}$ reaction, using a radioactive ^{17}F beam and a 100 μg/cm^2 CH_2 target at the HRIBF. Recoiling ^{14}O ions were detected in coincidence with α

particles in the SIDAR: the heavy particles were detected at lab angles of 3.2° to 6.5° in a small, 64-segment annular detector while the alphas were detected at lab angles of 10° – 25° in two stacked rings of eight 16-segment annular detectors (Figure 1.a).

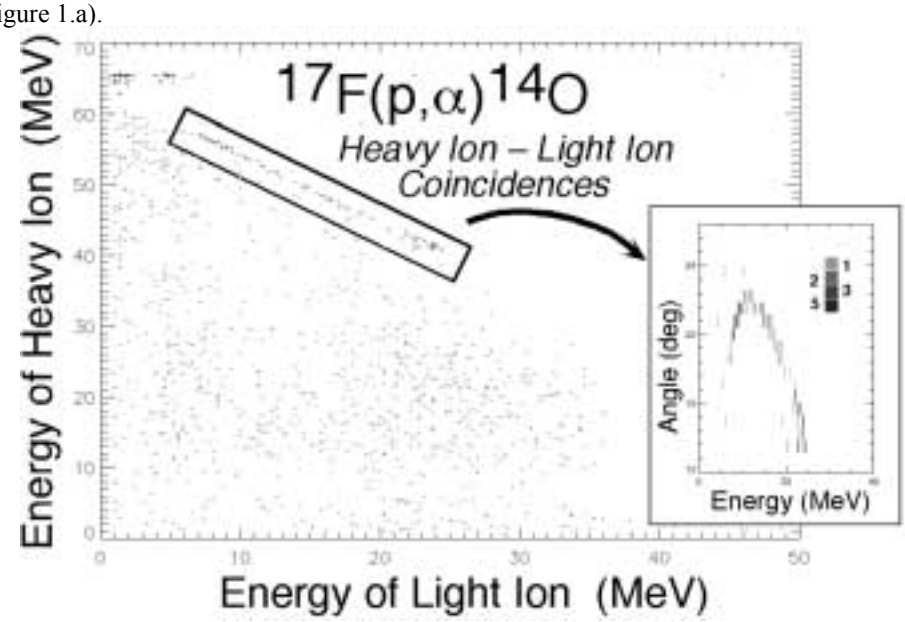

Figure 3. Energy – Energy plot used to identify $^{14}O - \alpha$ coincidences in a measurement of the $^{17}F(p,\alpha)^{14}O$ reaction, and the gated angle – energy plot of the α particles.

Stacking the detectors enabled $\Delta E - E$ particle identification which, along with gating on the energies of the ^{14}O and α particles as well as the energy–angle relationship of the alphas (Figure 3), enabled us to distinguish the weak $^{1}H(^{17}F,\alpha)^{14}O$ channel from an intense background from $^{17}F + ^{12}C$ fusion evaporation. The beam current, up to $2 \cdot 10^{6}$ s^{-1} on target, was determined by measuring $^{17}F + ^{12}C$ elastic scattering. An excitation function of the $^{1}H(^{17}F,\alpha)^{14}O$ reaction was determined by measuring the absolute cross section at 21 energies, covering for the first time the entire energy range of interest for $^{14}O(\alpha,p)^{17}F$ (E_{α}^{cm} = 1.0 - 2.6 MeV). The cross section varied by a factor of ~10^{3} over this energy range, and the $\alpha - ^{14}O$ coincidence rate varied from ~1 min^{-1} to 2 day^{-1}. Properties of states in ^{18}Ne with excitation energies E_x = 6.0-7.7 MeV are currently being determined from our data, including the important $J^{\pi} = 1^{-}$ state. The non-resonant reaction cross section and its interference with the 1^{-} resonance were also measured. This will enable the $^{14}O(\alpha,p)^{17}F_{gs}$ reaction rate to be determined with reasonable certainty for the first time covering temperatures important for novae and X-ray bursts.

4.2 The $^{17}F(p,\gamma)^{18}Ne$ Reaction

The $^{17}F(p,\gamma)^{18}Ne$ reaction rate was uncertain because of a 3^+ state that was known in the analog nucleus ^{18}O [36] but never conclusively observed in ^{18}Ne. This missing 3^+ state would provide a strong s-wave ($\ell = 0$) resonance and, depending on its excitation energy, could dominate the $^{17}F(p,\gamma)^{18}Ne$ reaction rate at temperatures corresponding to stellar explosions [37].

Three calculations of the properties of this state differed by a factor of 8 in total width and by 314 keV in excitation energy [37-39]. Nine previous studies of this excitation energy range in ^{18}Ne found no conclusive evidence for the existence of the 3^+ state, including recent measurements of $^{16}O(^3He,n)^{18}Ne$ [38] and high precision measurements of $^{20}Ne(p,t)^{18}Ne$ [40,41]. These efforts were hindered by using reactions that suppress the population of states with unnatural spin and parity (such as the 3^+). The uncertainty in the $^{17}F(p,\gamma)^{18}Ne$ reaction rate was as large as a factor of 100 based on theoretical estimates of properties of this resonance. To resolve this uncertainty, we measured the $^1H(^{17}F,p)^{17}F$ excitation function with a radioactive ^{17}F beam at the HRIBF. This reaction is extremely sensitive to 2^+ and 3^+ states in ^{18}Ne, and our measurement provided the first unambigious evidence for the existence of the missing 3^+ state [42].

A ^{17}F beam with energies of 10 – 12 MeV, an average intensity of 8000 s^{-1}, and a typical ^{17}F to ^{17}O ratio of 1000 to 1, was used to bombard a 48 $\mu g/cm^2$ polypropylene CH_2 target. Scattered protons were detected in the SIDAR (at lab angles of 25 to 51 degrees) while recoil ^{17}F ions were detected in coincidence (with more than 90 % coincidence efficiency) in our isobutane-filled ionization counter. The setup was similar to that in Figure 1.b, but with the Si detectors normal to the beam axis. The beam current was determined by measuring $^{17}F + {}^{12}C$ elastic scattering. A total of only $2 \cdot 10^9$ ^{17}F ions over the duration of the experiment were needed for this measurement. Proton yields were determined at 12 beam energies (Figure 4) by summing the coincident proton yields in all strips of the SIDAR and normalizing to the same incident beam current. The coincidence requirement was used to eliminate background from e^+ particles arising from decay of scattered beam particles. A $^{17}F + p$ resonance structure is clearly visible in Figure 4, and a fit to the data yields a resonance energy of $E_{res} = 599.8 \pm 1.5$ (stat) $\pm$ 2.0 (sys) keV and a total width of $\Gamma = 18 \pm 2$ keV. We conclude that we have observed the long sought 3^+ state in ^{18}Ne for the following reasons: our measurement is sensitive to 3^+ and 2^+ states only; there are no 2^+ states in ^{18}O whose analogs have not been identified in ^{18}Ne; the observed width is consistent with the expected width of the 3^+ state but is five times larger than what is expected for a 2^+ state; and the angular distributions of the protons is consistent with a 3^+ assignment.

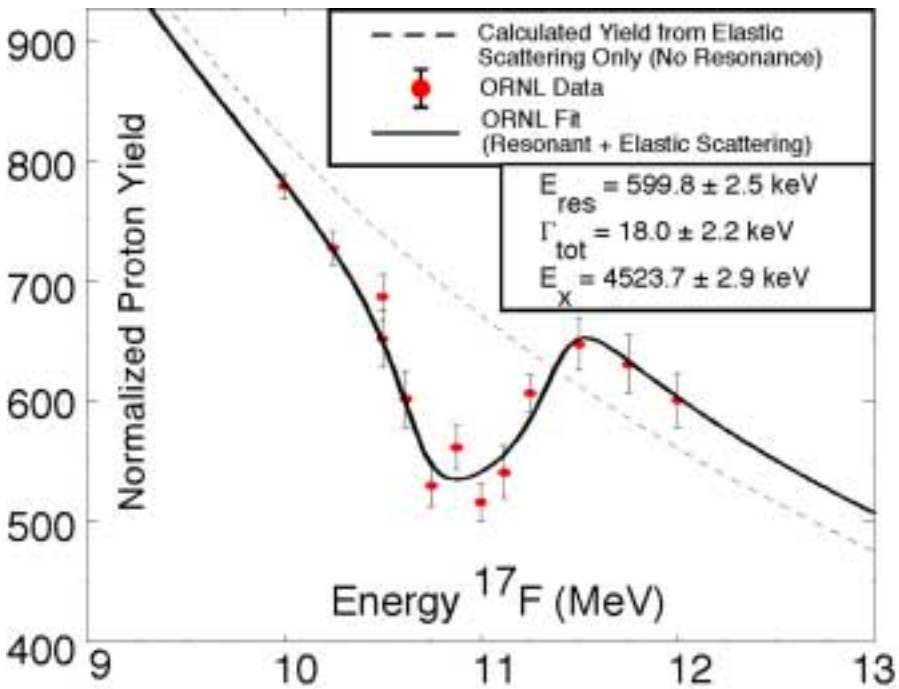

Figure 4. Excitation function for the $^{17}F(p,p)^{17}F$ reaction showing the $J^{\pi} = 3^{+}$ resonance at E_x = 4523.7 keV in Ne. The listed resonance properties were determined from a fit to the data.

Our discovery of the 3^{+} state resolves the greatest uncertainty in the $^{17}F(p,\gamma)^{18}Ne$ rate. This rate calculated with our new resonance parameters differs by up to a factor of 100 from some previous estimates. When inserted into a model of the synthesis of isotopes in an energetic nova explosion, the predicted production of some isotopes changed by more than a factor of 1000 when compared to predictions using the rate from [37]. However, the total $^{17}F(p,\gamma)^{18}Ne$ rate is still somewhat uncertain because the direct capture cross section and partial gamma width of the 3^{+} state have not been measured. These problems could be solved with the direct measurement of $^{17}F(p,\gamma)^{18}Ne$ planned at the HRIBF.

4.3 The $^{18}F(p,\alpha)^{15}O$ and $^{18}F(p,\gamma)^{19}Ne$ Reactions

Both the $^{18}F(p,\alpha)^{15}O$ and $^{18}F(p,\gamma)^{19}Ne$ reactions serve to destroy any ^{18}F nuclei which could (via their radioactive decay) be observables in novae ejecta, and the former reaction is thought to be ~ 500 times faster than the latter [43]. Both reactions are possibly dominated at nova temperatures by a ^{19}Ne resonance near E_x = 7.07 MeV – depending on its properties. Recent experimental results [26, 43-46] have differed by up to a factor of three in their adopted (p,α) resonance strength and by as much

as 21 keV in their excitation energy for this state. This results in up to a factor of three variation in the $^{18}F(p,\alpha)^{15}O$ rate at stellar explosion temperatures. To resolve these discrepancies, we measured the $^{1}H(^{18}F,p)^{18}F$ and $^{1}H(^{18}F,\alpha)^{15}O$ excitation functions with a thin (35 $\mu g/cm^2$) CH_2 target and a radioactive ^{18}F beam at the HRIBF. Proton and alpha yields were measured in coincidence in the SIDAR with the heavy recoil nuclei at fifteen bombarding energies from 10 - 14 MeV. Six 16-segment silicon strip detectors were configured to face towards the beam axis (Figure 1.b) for a larger solid angle coverage than used in our $^{1}H(^{17}F,p)^{17}F$ measurement [42]. In the $^{1}H(^{18}F,\alpha)^{15}O$ measurement, the ^{15}O particles were detected in the inner strips of the array (small angles from the beam axis), while the α particles were detected in coincidence in the outer strips (larger angles). Preliminary analysis suggests that we can extract the width of the E_x = 7.07-MeV resonance to 5 keV, the resonance energy to 1 keV, and the proton-width to α-width ratio to 5 %.

5 Other Astrophysics Research at ORNL

In addition to the measurements with radioactive beams described above, there are a number of other astrophysics research efforts at ORNL - in theoretical astrophysics, nuclear astrophysics data evaluation, heavy element nucleosynthesis measurements, theoretical atomic astrophysics, and atomic astrophysics data. The first two of these research programs are closely coupled to the HRIBF measurement program, and are briefly described in the following subsections.

5.1 Theoretical Astrophysics

A new program at ORNL in theoretical and computational astrophysics has as one of its foci the study of stellar explosions and explosive nucleosynthesis. One of the main areas of research is the core collapse supernova mechanism. Simulations in one-, two-, and three-dimensions focusing on issues of exact (Boltzmann) neutrino transport, convection, and their interplay in the explosion mechanism, are being carried out on supercomputers [47 - 49]. Another research effort is under way to model abundance yields in nova explosions, and to quantitatively determine the contributions of nuclear reaction rate uncertainties on the predictions of nova models. We are carrying out the first systematic analyses of the impact of all reaction rate uncertainties considered simultaneously on nova nucleosynthesis [50]. We are also determining the correlation between the uncertainties of individual rates with the production uncertainties of individual isotopes. This will enable us to make quantitative comparisons between theory and observations, as well as to determine the relative importance of changes in individual reaction rates and provide guidance in the selection of reactions for further experimental study. This work is closely

coupled to the HRIBF experimental measurement program and to the nuclear astrophysics data work described below.

5.2 Nuclear Astrophysics Data

Computer models of stellar explosions, as well as models of other astrophysical phenomena, require a very diverse set of nuclear physics information to determine the synthesis of isotopes and the energy released from nuclear reactions. There is a substantial need for more complete, precise, and timely evaluations of nuclear properties needed for astrophysical models [51]. A number of projects are underway to meet the nuclear astrophysics data needs of the ORNL experimental and theoretical nuclear astrophysics research programs. For example, to prepare for measurements of $^{14}O(\alpha, p)^{17}F$ and $^{17}F(p, \gamma)^{18}Ne$, we evaluated the rates of these reactions determined from indirect experimental measurements [52]. Similarly, evaluations $^{18}F(p, \gamma)^{18}Ne$ and $^{18}F(p, \alpha)^{15}O$ are in progress, as are evaluations of $^{17}O(p, \gamma)^{18}F$ and $^{17}O(p, \alpha)^{14}N$ – the latter two reactions to help understand the production of oxygen isotopes in Red Giant Stars. Rates for these reactions are being determined with uncertainties, in formats that can be readily input into reaction rate network codes, and will be posted on the WWW. Another project addressed the need to easily (i.e., electronically) incorporate the 160 thermonuclear reaction rates (and their inverses) in the Caughlan and Fowler 1988 reaction rate collection [53] into computer models. We prepared the first electronic dissemination of this extremely valuable rate collection in the form of a downloadable FORTRAN subroutine [54]. Tabular data for these rates and plots of rates versus temperature have been added, along with a graphical search engine based on the chart of the nuclides and the temperature derivatives of these rates – useful for coupling nucleosynthesis calculations to hydrodynamics. Another data project involved compiling a nuclear astrophysics data bibliography, with over 1200 references, that is posted on the WWW [54].

6 Summary

Measurements of capture reactions on proton-rich radioactive isotopes are crucial to the understanding of explosive nucleosynthesis occurring in stellar explosions such as novae and X-ray bursts. We have recently measured the $^{17}F(p,p)$, $^{17}F(p,\alpha)^{14}O$, $^{18}F(p,p)$, and $^{18}F(p,\alpha)^{15}O$ reactions at ORNL's Holifield Radioactive Ion Beam Facility with a Silicon Detector Array (SIDAR) to better understand these explosions. The Daresbury Recoil Separator (DRS) has also been installed at HRIBF and is being readied to study capture reactions in inverse kinematics. Initial tests with stable beams indicate that the DRS gives an excellent suppression of scattered beam particles in these reactions. Additionally, there are theoretical

astrophysics and nuclear astrophysics data evaluation work at ORNL which are closely coupled to the HRIBF experimental nuclear astrophysics work.

7 Acknowledgements

The author wishes to thank D.W. Bardayan and D.C. Larson for helpful comments. RIBENS (Radioactive Ion Beams for Explosive Nucleosynthesis Studies) collaboration members D.W. Bardayan, J.C. Blackmon, W. Bradfield-Smith, C. R. Brune, A.E. Champagne, A. Chen, T. Davinson, U. Greife, K.I. Hahn, V. Hansper, M. Hofstee, A.N. James, B.A. Johnson, P.E. Koehler, R.L. Kozub, C.S. Lee, R. Lewis, Z. Ma, P.D. Parker, D.E. Pierce, G. Rajbaidya, R.C. Runkle, C.M. Rowland, A.C. Shotter, M.S. Smith, F. Strieder, K.B. Swartz, D.W. Visser, and P.J. Woods contributed to the HRIBF measurements, along with T.A. Lewis, J.W. McConnell, W.T. Milner, and D. Shapira. The theoretical collaborators were W.R. Hix, A. Mezzacappa, S. Starrfield, and D.L. Smith. ORNL is managed by UT-Battelle, LLC for the U.S. Dept. of Energy under contract DE-AC05-00OR22725.

References

1. R.K. Wallace and S.E. Woosley, *Ap. J. Suppl*. **45** (1981) 389.
2. A.E. Champagne and M. Wiescher, *Ann. Rev. Nucl. Part. Sci.* **42** (1992) 39.
3. K. M. Vanlandingham et al., *Mon. Not. R. Aston. Soc.* **282** (1996) 563.
4. Y. Chin, C. Henkel, N. Langer, R. Mauersberger, *Ap. J. Lett.* **512** (1999) L143.
5. S.A. Glasner, E. Livne, and J.W. Truran, *Ap. J.* **475** (1997) 754.
6. S. Shore et al., *Ap. J.* **421** (1994) 344.
7. J. Gomez-Gomar, M. Hernanz, J. Jose, and J. Isern, *Mon. Not. R. Aston. Soc.* **296** (1998) 913.
8. M. J. Harris et al., *Ap. J*, **522** (1999) 424.
9. M. Hernanz et al., *Ap. J*. **526** (1999) L97.
10. M. Wiescher, J. Goerres, F.-K. Thielemann, and H. Ritter, *Astron. Astrophys*. **160** (1986) 563.
11. Jose et al., A. Coc, and M. Hernanz, *Ap. J.* **520** (1999) 347.
12. S. Starrfield et al., *Mon. Not. R. Aston. Soc.* **296** (1998) 502.
13. S. Starrfield, *Phys. Rept.* **311** (1999) 371.
14. R.E. Taam, S.E. Woosley, T.A. Weaver, D.Q. Lamb, *Ap. J.* **413** (1993) 324.
15. H. Schatz, L. Bildsten, A. Cumming, and M. Wiescher, *Ap. J.* **524** (1999) 1014.
16. H. Schatz et al., *Phys. Rept.* **294** (1998) 167.
17. M. Wiescher, H. Schatz, and A.E. Champagne, *Philos. Trans. R. Soc. London* **A356** (1998) 2105.
18. O. Koike, M. Hashimoto, K. Arai, and S. Wanajo, *Astron. Astrophys*. 342 (1999) 464.
19. K. Arai, M. Hashimoto, *Astron. Astrophys.* **254** (1992) 191.

20. M. Wiescher, J. Gorres, H. Schatz, *J. Phys.* **G 25** (1999) R133.
21. G.D. Alton and J.R. Beene, *J. Phys.* **G 24** (1998) 1347.
22. G.D. Alton, J.R. Beene, and Y. Liu, *Nucl. Inst. Meth.* **A438** (1999) 190.
23. R.F. Welton et al., *Nucl. Inst. Meth.* **B159** (1999) 116.
24. G.D. Alton, Y. Liu, C. Williams, and S.N. Murray, *Proc. Eighth Int. Conf. Heavy Ion Accelerator Technology*, ed. K.W. Shepard, (1999) p. 330.
25. P.J. Sellin et al., *Nucl. Inst. Meth.* **A311** (1992) 217.
26. R. Cozach et al., *Phys. Letts.* **B353** (1995) 184.
27. D.W. Bardayan, *Applications of Accelerators in Research and Industry*, eds. J.L. Duggan, I.L. Morgan, AIP: New York, 1999, p. 326.
28. A.N. James et al., *Nucl. Inst. Meth.* **A267** (1988) 144.
29. M.S. Smith et al., in *Stellar Evolution, Stellar Explosions, and Galactic Chemical Evolution*, ed. A. Mezzacappa, IOP: Bristol, 1998, p. 511**.**
30. M.S. Smith, in *Proc. Origin Matter Evolution Galaxies 97*, eds. S. Kubono, T. Kajino, K.I. Nomoto, I. Tanihata, World Scientific: Singapore, 1998, p. 200.
31. M.S. Smith, C. Rolfs, and C.A. Barnes, *Nucl. Inst. Meth.* **A306** (1991) 233.
32. L. Gialanella et al., *Nucl. Inst. Meth* . **A376** (1996) 174.
33. C. Funck and K. Langanke, Nucl. Phys. **A480** (1988) 188.
34. K. I. Hahn et al., *Phys. Rev.* **C54** (1996) 1999.
35. B. Harss et al., *Phys. Rev. Lett.* **82** (1999) 3964.
36. D.R. Tilley, H.R. Weller, C.M. Cheves, and R.M. Chasteler, *Nucl. Phys.* **A595** (1995) 1.
37. M. Wiescher, J. Gorres, R.-K. Thielemann, *Ap. J.* **326** (1988) 384.
38. A. García et al., *Phys. Rev.* **C43** (1991) 2012.
39. R. Sherr and H.T. Fortune, *Phys. Rev.* **C58** (1998) 3292.
40. K. I. Hahn et al., *Phys. Rev.* **C54** (1996) 1999.
41. S.H. Park et al., *Phys. Rev*. **C59** (1999) 1182.
42. D.W. Bardayan et al., *Phys. Rev. Lett.* **83** (1999) 45.
43. S. Utku et al., *Phys. Rev.* **C57 (**1998) 2731.
44. J.S. Graulich et al., *Nucl. Phys.* **A626** (1997) 751.
45. K.E. Rehm et al., *Phys. Rev.* **C52** (1995) R460; **C53** (1996) 1950; **C55** (1997)**.**
46. J.S. Graulich, Ph.D. Thesis (in preparation).
47. O.E.B. Messer et al., *Ap. J.* **507** (1998) 353.
48. A. Mezzacappa et al., *Ap. J.* **493** (1998) 848.
49. A. Mezzacappa et al., *Ap. J.* **495** (1998) 911.
50. W.R. Hix, M.S. Smith, A. Mezzacappa, S. Starrfield, in *Cosmic Explosions, a Conference Proceedings*, ed. S.S. Holt, AIP: Melville (2000) in press.
51. M.S. Smith et al., http://www.phy.ornl.gov/astrophysics/data/task/taskforce_report.html.
52. D.W. Bardayan and M.S. Smith, *Phys. Rev.* **C56** (1997) 1647.
53. G.R. Caughlan, W.A. Fowler, *At. Data Nucl. Data Tables* **40**, (1988) 283.
54. M.S. Smith et al., ORNL Nuclear Astrophysics Data Website: http://www.phy.ornl.gov/astrophysics/data/data.html.